COMPONENT PART NOTICE

THIS PAPER IS A COMPONENT PART OF THE FOLLOWING COMPILATION REPORT:

TITLE: Ceramic Transactions. Volume 21. Proceedings of the Symposium on

Microwave Theory and Application in Materials Processing Annual

Meeting of the American Ceramic Society (23rd) Held in Cincinnatti, OH

on April 29-May 3, 1991.

TO ORDER THE COMPLETE COMPILATION REPORT, USE __AD-A253 631__.

THE COMPONENT PART IS PROVIDED HERE TO ALLOW USERS ACCESS TO INDIVIDUALLY
AUTHORED SECTIONS OF PROCEEDING, ANNALS, SYMPOSIA, ETC. HOWEVER, THE COMPONENT
SHOULD BE CONSIDERED WITHIN THE CONTEXT OF THE OVERALL COMPILATION REPORT AND
NOT AS A STAND-ALONE TECHNICAL REPORT.

THE FOLLOWING COMPONENT PART NUMBERS COMPRISE THE COMPILATION REPORT:

AD#: __AD-P007 716__   thru AD#: __P007 783__

AD#: _____   AD#: _____

AD#: _____   AD#: _____

DTIC
ELECTE
AUG 13 1992
S   D

DTIC QUALITY INSPECTED 5

Accession For	
NTIS GRA&I	☑
DTIC TAB	☐
Unannounced	☐
Justification	

By_____
Distribution/
Availability Codes

Dist	Avail and/or Special
A-1	

PARAMETRIC EXPERIMENTAL STUDY OF MICROWAVE ABSORPTION IN CHIRAL COMPOSITES

Ruyen Ro, Vasundara V. Varadan and Vijay K. Varadan
Center for the Engineering of Electronic and Acoustic Materials &
Department of Engineering Science and Mechanics
The Pennsylvania State University
University Park, PA 16802

ABSTRACT

Theoretical and experimental studies have shown that chiral composites constructed by embedding chiral inclusions in an otherwise achiral lossy medium enhance power absorption in the microwave frequency range. Chiral composites can hence be used as microwave absorbers to achieve rapid heating during microwave processing of ceramics, glass, and composites. Power absorption bands of chiral composites are discussed and the corresponding ratio of the one turn length of the chiral inclusion to the wavelength in the medium L/λ_c are reported. This ratio can be used to optimize absorption at different operating frequencies. Experimental studies on chiral composites having different sizes of chiral inclusions are also included.

INTRODUCTION

In recent years, the exploitation of microwave energy in thermal processing of materials has caused great interest [1]. The prevalent applications of microwave power have been seen in the dehydration of various materials and in the processing of ceramics, glass and composites [2, 3, 4]. The major advantages of the microwave heating are: 1) high heating rates can be obtained because of microwave absorption inside the material 2) energy can be applied or removed instantly and 3) the heating is volumetric rather than surface heating. The fundamental principle of applying microwave powers in materials processing is due to loss mechanisms (dielectric and magnetic) in the material during the interaction of electromagnetic waves. Since many ceramics are difficult to heat using microwave power due to their low dielectric loss tangent at room temperature, the microwave processing of ceramics is limited to those which have a high dielectric loss tangent. However, with the help of a sealing agent or interlayer which exhibits microwave absorption properties, microwave sealing or joining of ceramics is possible. For example,

coupling agents such as SiC and Si_3N_4 whiskers have been used to couple electromagnetic waves for microwave sintering of the matrix materials Al_2O_3-SiC and ZrO_2-Si_3N_4, which are transparent to microwave energy [5]. Recently, the research group at Penn State has discovered theoretically and experimentally that chiral composites can enhance microwave absorption [6, 7, 8, 9]. Due to recent progress in the construction of artificial composites and synthesis of polymers, it is feasible to design artificial chiral composite materials consisting of specified materials. Lately, we have developed a method for determining the electromagnetic properties of chiral composite materials in the frequency range 8-40 GHz [10]. It is also important to investigate the power absorption bands of chiral composites not only for confirming the "Cotton effect" phenomenon [11] but also for designing chiral composites as microwave absorbers. From electromagnetic properties of chiral composites, the ratio of the one turn length of the chiral inclusion to the wavelength in the chiral medium which maximizes power absorption can be calculated and will be examined in this study.

Optical activity and chirality have been observed for almost two centuries. The twin phenomena, optical rotation dispersion (ORD) and circular dichroism (CD), are the special features of optically active media. They can be explained by directly substituting new constitutive relations, e.g., $D = \epsilon E + \beta \epsilon \nabla \times E$ and $B = \mu H + \beta \mu \nabla \times H$, into Maxwell's equations [8, 12]. Here, ϵ and μ are the complex permittivity and permeability, respectively, while β is the complex chirality parameter which results from any chirality (handedness) in the microstructure of the medium. For a normally incident, linearly polarized wave, the transmitted wave traveling through the chiral medium is not only rotated but becomes elliptically polarized due to the existence of the chirality parameter [8, 10]. This results from the different phase velocities and different absorption for the left- and right-circularly polarized waves. The reflected wave, however, is linearly polarized for a normally incident, linearly polarized wave. Hence, one reflection and two transmission measurements are needed to fully characterize the chiral composite [10].

The planar chiral composites characterized in this study were constructed by embedding chiral inclusions (helices) into an otherwise achiral host medium (Eccogel). Samples made in this research have the dimensions 15 cm × 15 cm × 1.2 cm. For detailed information on how the samples are made, refer to Guire *et al.* [9]. A free-space measurement setup was employed to measured the reflection and transmission characteristics of the chiral composites. The calibration technique and time domain gating for enhancing measurement accuracy, as well as the measurement procedure for the free-space measurement system are referred to Ghodgaonkar *et al.* [13].

ABSORPTION BANDS OF CHIRAL COMPOSITES

The time-averaged Poynting vector denoted by <P> represents the amount of power crossing a unit area in the direction perpendicular to both E and H fields and is defined by

$$<P> = \frac{1}{2} \text{Re} \, (E \times H^*) \qquad (1)$$

where Re means the 'real part of' and the asterisk denotes the complex conjugate. The electromagnetic fields ($\mathbf{E}$ and $\mathbf{H}$) in free-space can be expressed in terms of LCP (left-circularly polarized) and RCP (right-circularly polarized) waves Q_L and Q_R as

$$\mathbf{E} = \mathbf{Q}_L + \mathbf{Q}_R \tag{2a}$$

$$\mathbf{H} = \frac{i}{\eta_0}(-\mathbf{Q}_L + \mathbf{Q}_R) \tag{2b}$$

Substituting Eqs. (2a) and (2b) into Eq. (1), one can obtain

$$<P> = \frac{1}{2}\text{Re}\left\{\frac{1}{\eta_0}(\mathbf{Q}_L \times \mathbf{Q}_L^* - \mathbf{Q}_R \times \mathbf{Q}_R^*)\right\} \tag{3a}$$

and

$$P = |<P>| = \frac{c^2}{4\eta_0}\{S_L S_L^* + S_R S_R^*\} \tag{3b}$$

where C is the magnitude of the incident field $\mathbf{E}_{inc}$ and η_0 is the free-space impedance. S_L and S_R are either the reflection or transmission coefficients for the LCP and RCP waves, respectively. The reflection and transmission characteristics for the normally incident, circularly polarized waves can be obtained from the measured reflection and transmission characteristics for a normally incident, linearly polarized wave as

$$S_{11L} = S_{11R} = S_{11co} \tag{4a}$$

$$S_{21L} = S_{21co} - iS_{21cross} \tag{4b}$$

$$S_{21R} = S_{21co} + iS_{21cross} \tag{4c}$$

and

$$S_{21cross} = \frac{S_{21\alpha} - S_{21co}\cos\alpha}{\sin\alpha} \tag{4d}$$

where S_{11co} is the measured reflection coefficient and S_{21co} and $S_{21\alpha}$ are the measured transmission coefficients at co-polarization position and angle α from co-polarization position, respectively [10].

The power reflection ratio $R = P_{ref}/P_{inc}$ and power transmission ratio $T = P_{tra}/P_{inc}$ then can be calculated by

$$R = \frac{P_{ref}}{P_{inc}} = \frac{1}{2}\{S_{11L}S_{11L}^* + S_{11R}S_{11R}^*\} = S_{11co}S_{11co}^* \tag{5a}$$

and

$$T = \frac{P_{ref}}{P_{inc}} = \frac{1}{2} \{ S_{21L} S_{21L}^* + S_{21R} S_{21R}^* \} = S_{21co} S_{21co}^* + S_{21cross} S_{21cross}^* \qquad (5b)$$

Computations of the power absorption coefficient of the chiral composite

$$A = \frac{P_{inc} - P_{ref} - P_{tra}}{P_{inc}} = 1 - R - T \qquad (6)$$

can therefore be made.

The chiral inclusions used for determination of the properties have the dimensions diameter D = 0.11684 cm, pitch P = 0.0529 cm and one turn length L = 0.371 cm. From the reflection and transmission measurements S_{11co}, S_{21co}, and $S_{21\alpha}$, the electromagnetic properties of chiral composites ϵ, μ, and β can be calculated [10]. The wavenumbers for the LCP and RCP waves, k_L and k_R, as well as the wavelengths for the LCP and RCP waves, λ_L and λ_R, can then be obtained from these properties [8,10]. The ratios of the one turn length of the chiral inclusion to the wavelengths in the chiral medium, L/λ_L and L/λ_R, at each frequency for each sample then can be calculated. Table 1 shows peak values of power absorption coefficients, A, and the corresponding frequencies as well the corresponding ratios, L/λ_L and L/λ_R, for the chiral composites.

Table 1. Peak values of power absorption coefficients, A, and the corresponding frequencies as well as the corresponding ratios, L/λ_L and L/λ_R, of power absorption coefficients for the chiral composites.

Sample	Peak value	Frequency (GHz)	L/λ_L	L/λ_R
0.8% left	0.7626	28.86	0.596	0.610
0.8% right	0.7135	28.19	0.5933	0.578
0.8% racemic	0.7853	28.19	0.589	0.589
1.6% left	0.8516	26.84	0.556	0.588
1.6% right	0.9263	26.50	0.565	0.562
1.6% racemic	0.8491	27.51	0.585	0.585
3.2% left	0.9281	28.19	0.609	0.672
3.2% right	0.9881	31.23	0.742	0.693
3.2% racemic	0.9657	30.55	0.693	0.693

It can be seen in Table 1 that the peak frequencies for the same volume concentration samples are very close. For the 0.8% samples, the averaged peak frequency is 28.41 ± 0.446 GHz. While for the 1.6% and 3.2% samples, the averaged peak frequencies are 26.95 ± 0.56 GHz and 29.99 ± 1.24 GHz, respectively. The peak values of the power absorption coefficients are also very close for the same volume concentration samples, but vary as the volume concentrations change. The values are 0.7538 ± 0.0403, 0.876 ± 0.0503, and 0.9606 ± 0.0325 for the 0.8%, 1.6%, and 3.2% samples, respectively.

It also can be seen that the ratios L/λ_L and L/λ_R are different for handed (left- or right-) samples but are the same for the racemic samples. This is because LCP waves travel faster than RCP waves inside the left-handed medium, and *vice versa*, while both LCP and RCP propagate with the same speed inside the racemic samples [8]. Since the difference between L/λ_L and L/λ_R is less than 5% for every sample, one can use the average value of L/λ_L and L/λ_R as the ratio L/λ_c with an error of less than 3%. The ratio L/λ_c varies as the volume concentration changes. The values are 0.5926 ± 0.01, 0.5735 ± 0.0115, and 0.6837 ± 0.04 for the 0.8%, 1.6%, and 3.2% samples, respectively.

Table 2. 95% and 90% power absorption bandwidths.

Sample	95% peak value bandwidth (GHz)	90% peak value bandwidth (GHz)	Frequency (GHz)
0.8% left	26.50 ~ 31.56 5.06	25.23 ~ 32.58 7.35	28.86
0.8% right	25.01 ~ 30.55 5.54	24.59 ~ 31.56 6.97	28.19
0.8% racemic	25.65 ~ 29.54 3.89	23.31 ~ 30.55 7.24	28.19
1.6% left	22.46 ~ 31.23 8.77	21.82 ~ 32.24 10.42	26.84
1.6% right	25.01 ~ 29.88 4.87	22.04 ~ 32.24 10.20	26.50
1.6% racemic	25.23 ~ 31.23 6.0	22.25 ~ 32.58 10.33	27.51
3.2% left	26.29 ~ 32.91 6.62	25.01 ~ 35.61 10.60	28.19
3.2% right	26.29 ~ 37.30 11.01	25.23 ~	31.23
3.2% racemic	26.50 ~ 36.96 10.46	25.23 ~	30.55

Based upon the data shown in Table 1, the average value and standard deviation of the ratio L/λ_c are 0.6038 and 0.051, while for the peak frequency they are 28.45 and 1.4828 GHz. The variances of the peak frequency and the ratio L/λ_c among the same volume concentration chiral samples may be due to sample variations and post-calibration errors. Thus $L/\lambda_c = 0.6038$ can be used as a design criterion to obtain an absorption peak at a desired operating frequency.

It is also interesting to study the bandwidths of the power absorption coefficients. Table 2 shows the 95% and 90% peak values power absorption bandwidths for the chiral samples. The average bandwidths of 95% and 90% power absorption coefficients are 6.92 and 10.29 GHz, respectively. The smallest bandwidths for the 95% and 90% power absorption are 3.89 and 6.97 GHz, respectively. The corresponding changes for the ratios L/λ_c are 0.08 and 0.143, respectively. From this data, one can clearly see that the average values of the peak frequency 28.45 GHz and the ratio L/λ_c 0.6038 are within the 95% power absorption bandwidths region for each chiral sample. Hence, for this special kind of helix embedded into an epoxy host medium (Eccogel), it is appropriate to use the average values of the peak frequencies and the ratio L/λ_c of these nine chiral composites to represent the characteristic peak frequency 28.45 GHz and the ratio ratio L/λ_c 0.6038.

PARAMETRIC EFFECTS OF CHIRAL COMPOSITES

In addition to the one kind of helix as discussed above, three different geometrical dimensions of helices have been selected to examine the parametric effects of chiral inclusions. Four additional 3.2% left-handed samples have been made. One of them contains all four different geometrical sizes of chiral inclusions, which have been mixed well. The other three samples have only one kind of helix. Detailed description of the samples and the dimensions of helices are shown in Table 3.

The reflection and transmission characteristics for these samples may be measured in the frequency range 8-40 GHz by employing the free-space measurement system. The transmission coefficients of some samples, especially for samples C, D, and E, are less than – 40 dB at certain frequencies. This is very close to the dynamic range of the free-space measurement system, hence, it is improper to use these values to determine the properties of samples.

However, the power absorption of samples can also be seen from the reflection coefficients with metal backing. Fig. 1 shows the measured reflection coefficients with metal backing for each sample. It can be seen that the reflection coefficient for sample D has the largest value over the whole frequency range, probably due to the big impedance mismatch caused by variations of sample preparations. The reflection coefficient of sample E has not only the smallest value in the frequency range of 12-37 GHz but also the widest power absorption bandwidth. Since each kind of helix may have its power absorption peak frequency and bandwidth separately, e.g., 28.45 GHz peak frequency and 6.92 GHz 95% power absorption bandwidth for sample A, then combinations of different kinds of helices may cause the power absorption bandwidth to increase. The increase in the power absorption for sample E may be due to the impedance match for the free-space or the interaction between each different kind of helix. However, no conclusion should

be made until more is known about the effects of the dimensions of the helix and the host material.

Table 3. Description of the samples and the dimensions of helices.

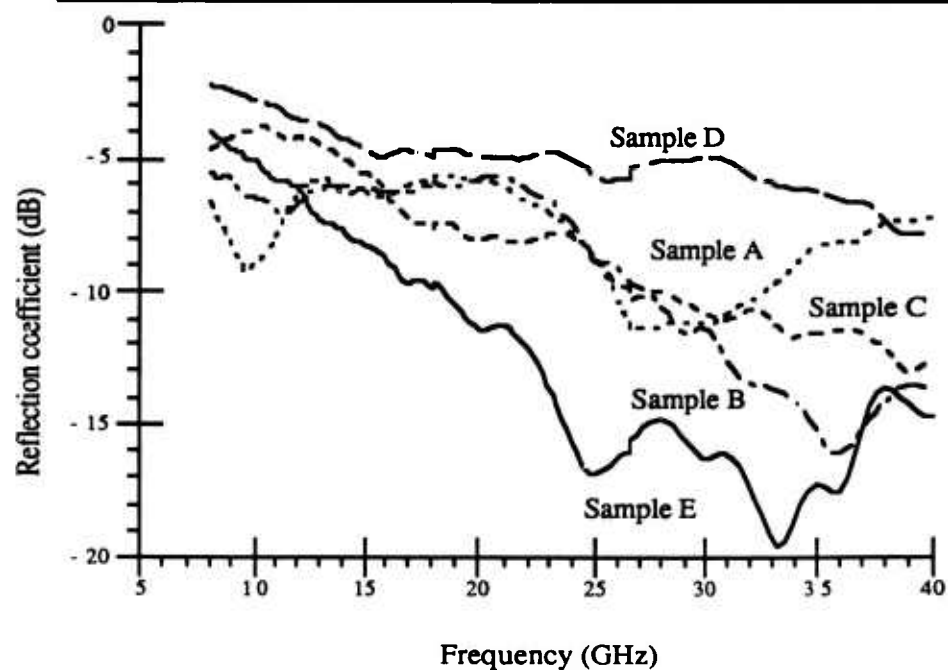| Name	Dimensions of the helix (cm)			
	Diameter D	Pitch P	One turn length L	No. of turns
Sample A	0.11684	0.0529	0.371	3
Sample B	0.11684	0.0794	0.3755	3
Sample C	0.18288	0.0529	0.577	3
Sample D	0.11176	0.254	0.433	3
Sample E	Mixed			

Fig. 1. The reflection coefficient with metal backing for each sample.

CONCLUSION

The power absorption bandwidths and the corresponding ratios L/λ_c of the one turn length of the chiral inclusion to the wavelength in chiral media have been examined. We have discovered that it is appropriate to use the averaged power absorption peak frequency and the corresponding ratio L/λ_c of different handed and different volume concentrations chiral samples to represent the characteristic peak frequency and the corresponding ratio L/λ_c of each chiral sample. Also, both the power absorption peak value and its bandwidth increase for the mixed sample compared with the samples which consist of only one kind of chiral inclusion. Thus the bandwidth of the absorption peak can be increased by considering inclusions with appropriate L/λ_c values at the frequencies in the band of interest. Such absorbers can then be used as the interlayer or heating catalyst in the joining and processing respectively of ceramics.

REFERENCES

[1]. W. H. Sutton, M.H. Brooks, and I.J. Chabinsky (Eds.), *Microwave processing of materials*, Materials Research Society Symposium Proceedings, Vol. 124, Pittsburgh, Material Research Society, 1988.

[2]. W.R. Tinga and W.A.G. Voss, *Microwave power engineering*, Academic Press, New York, 1968.

[3]. M.P. Borom and M. Lee, *Adv. Cerem. Mater.* 1, 335, 1986.

[4]. T.T. Meek, *J. Mater. Sci.* 6, 638, 1984.

[5]. Blake, R.D. and Meek, T.T., *Chapman and Hall Ltd.*, 1097-1098, 1986.

[6]. A. Lakhtakia, V.V. Varadan, and V.K. Varadan, *IEEE Trans. EMC.*, Vol. 28, No. 2, 90-95, 1986.

[7]. V.K. Varadan, V.V. Varadan, and A. Lakhtakia, *J. Wave-Material Interaction*, Vol. 2, No. 1, 71-81, 1987.

[8]. A. Lakhtakia, V.K. Varadan, and V.V. Varadan, *Time-harmonic electromagnetic fields in chiral media*, Springer-Verlag, Vol. 335, New York, 1989.

[9]. T. Guire, V.V. Varadan, and V.K. Varadan, *IEEE Trans. EMC.*, Vol. 32, 300-304, 1990.

[10]. V.V. Varadan, V.K., Varadan, R. Ro, and M. Umari, presented at the 1990 URSI Radio Science Meeting, Paper No. 36-1, Dallas, Texas, MAy 7-11, 1990.

[11]. P. Crabbe and S.A. Syntex, *Optical rotatory dispersion and circular dichroism in organic chemistry*, Holden-day, San Francisco, 1965.

[12]. C.F. Bohren, *Chemical Physics Letters*, Vol. 29, 458-462, 1974.

[13]. D.K. Ghodgaonkar, V.V. Varadan, and V.K. Varadan, *IEEE Trans. IM.*, Vol. 39, 387-394, 1990.